

# Fully Bridged Triphenylamine Derivatives as Color-Tunable Thermally Activated Delayed Fluorescence Emitters

Sheng-Nan Zou,<sup>‡</sup> Chen-Chen Peng,<sup>‡</sup> Sheng-Yi Yang, Yang-Kun Qu, You-Jun Yu, Xing Chen, Zuo-Quan Jiang,\* and Liang-Sheng Liao\*



Cite This: *Org. Lett.* 2021, 23, 958–962



Read Online

ACCESS |



Metrics & More

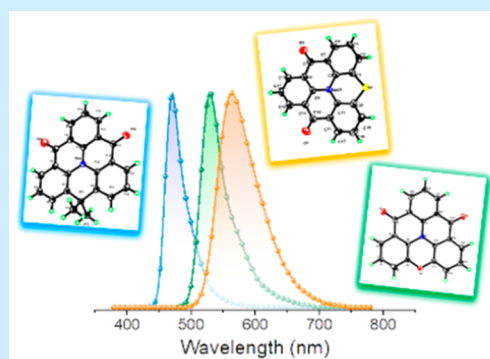


Article Recommendations



Supporting Information

**ABSTRACT:** Three emissive bridged-triphenylamine derivatives are designed and synthesized by incorporating carbon (DQAO), oxygen (OQAO), and sulfur (SQAO) atoms with two carbonyl groups. The fully bridged geometry and unique frontier molecular orbital distribution reveal its potential as narrowband thermally activated delayed fluorescence emitters. DQAO-, OQAO-, and SQAO-based organic light-emitting diodes exhibit the maximum external quantum efficiency (EQE<sub>max</sub>) of 15.2%, 20.3%, and 17.8% for blue, green, and yellow, respectively.



Triphenylamine, which carries a lone pair of electrons, acts as the classic skeleton in organic optoelectronics.<sup>1</sup> Thus, compounds possessing such moiety are generally electron-rich and triphenylamine had been readily employed as hole transport materials in organic light-emitting diodes (OLEDs), organic photovoltaics, or perovskite solar cells.<sup>2–6</sup> To further explore the potential of triphenylamine, the structural constraint, such as partially or fully bridged derivatives, is a sophisticated strategy to alter the fundamental nature of the parent molecule.<sup>7</sup> In 1971, Hellwinkel et al. first realized the nitrogen-centered triangulene HTANGO, which bears three carbonyl bridges. The distance of plane-to-plane is 3.46 Å in the single crystal, indicative of strong  $\pi$ - $\pi$  stacking interaction among the heterotriangulenes.<sup>8,9</sup> After three years, they further reported the dimethylmethylene-bridged derivatives.<sup>10</sup> In 2003, Venkataraman et al. expanded a series of partially carbonyl-bridged triphenylamines derivatives, which presented helically chiral conformations in the crystalline state and strong fluorescent emission in the blue region.<sup>11</sup> In 2005, Okada et al. prepared the oxygen-bridged triphenylamine, and its corresponding radical cation salt would be used in electronic and magnetic materials.<sup>12</sup> These studies reveal that a more planarized structure in triphenylamine derivatives can increase the interaction between  $\pi$ -skeletons and induce considerable oscillator strength for improved photophysical properties.

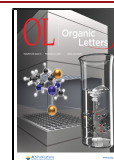
However, previous bridged triphenylamine derivatives in electroluminescence were not extensively explored. In 2019, our group first disclosed the potential application of 2-fold carbonyl-bridged triphenylamine QAO and its derivatives in OLEDs as the thermally activated delayed fluorescence

(TADF) emitters.<sup>13</sup> Unlike the conventional TADF compounds, its special frontier molecular orbital (FMO) distribution resulted from the donor-nitrogen atom and acceptor-carbonyl group, which generates effective short-range intramolecular charge transfer (ICT) assisting reverse intersystem crossing (RISC).<sup>14–21</sup> Intriguingly, owing to the rigid framework, its structure relaxation between the ground and twist induced excited states was suppressed. QAO is able to exhibit attractively narrow full width at half-maximum (fwhm) of 39 nm in sky blue and high external quantum efficiency (EQE) of 19.4% of OLEDs. This work demonstrates that the bridged carbonyl groups instead of the embed borane as electron accepting units could also achieve multiple resonance TADF (MR-TADF) as proposed by Hatakeyama's group.<sup>15</sup> Since the TADF emitters with narrow fwhm are highly demanded currently but color-tunable system has been rarely conducted.<sup>19,22</sup> Therefore, it is promising to develop more bridged-triphenylamine cases for OLED applications.

By embedding carbon, oxygen, and sulfur atoms into the third bridging position of N/C=O-based molecule QAO, three fully bridged-triphenylamine derivatives, 12,12-dimethyl-4H-benzo[9,1]quinolizino[3,4,5,6,7-defg]acridine-4,8(12H)-dione (DQAO), benzo[9,1]quinolizino[3,4,5,6,7-klmn]-

Received: December 16, 2020

Published: January 13, 2021



phenoxazine-8,12-dione (OQAO), and benzo[9,1]quinolizino[3,4,5,6,7-*klmn*]phenothiazine-8,12-dione (SQAO), were designed and synthesized (Figure 1). Among them, the sulfur-

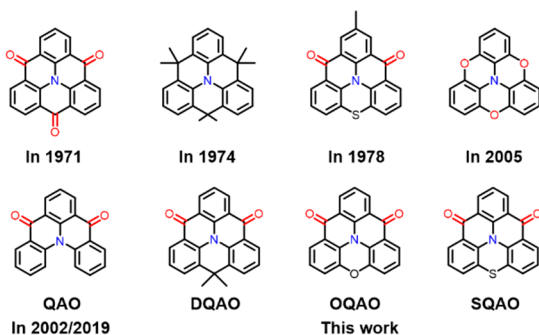


**Figure 1.** Some reported bridged triphenylamine derivatives and this work.

bridged scaffold, yet bearing one methyl group, could be dated back to 1978.<sup>23</sup> Their properties such as the arrangement of single crystals, energy bandgap, and thermal stability were adjusted by altering the substituent at the bridging positions. Eventually, three TADF emitters-based OLED showed significantly different emission wavelengths from blue to yellow region. In particular, the fwhm of DQAO-based and OQAO-based devices are as small as 34 and 45 nm, respectively. This work shows the tunability of the fully bridged triphenylamine strategy in designing TADF emitters.

The synthetic routes for DQAO, OQAO, and SQAO are summarized in Scheme S1. Precursor dimethyl 2-bromoisophthalate was prepared using a previous synthetic procedure in 72% yield in two steps.<sup>24</sup> Furthermore, the coupling of **3** with 9,10-dihydro-9,9-dimethylacridine, 10*H*-phenoxazine, and 10*H*-phenothiazine via copper-catalyzed Ullmann amination to give compounds **4**, **5**, and **6** in 72%, 68%, and 71% yield, respectively. Subsequent ester hydrolysis of **4**, **5**, and **6** in the presence of NaOH gave diacids **7**, **8**, and **9** in 96%, 94%, and 92% yield, respectively. Ultimately, the diacids **7**, **8**, and **9** were converted to the corresponding acid chloride with SOCl<sub>2</sub> in dichloromethane, followed by an in situ intramolecular cyclization in the presence of SnCl<sub>4</sub> to form triphenylamine derivatives DQAO, OQAO, and SQAO in 88%, 87%, and 91% yield. All the intermediates and target compounds were characterized by NMR, mass spectra, and elemental analysis (Figures S1–S27).

The molecular structures of DQAO, OQAO, and SQAO were further confirmed by the X-ray diffraction analysis (Figure 2 and Table S1–S6), and the crystal systems of the three compounds are all monoclinic lattices. Different from the helical structure of QAO (Figure S28), three molecules adopt the near trigonal-planar geometries and  $\pi$ -stacked with interplanar distances between 3.347 and 3.392 Å. Interestingly, the C–O–C bond angle of OQAO is 117.8(4)°, which is larger than C–C–C bond angle of 111.01(15)° in DQAO and C–S–C bond angle of 101.8(2)° in SQAO, and the C–C, C–O, and C–S lengths were found to be 1.520(2), 1.385(6), and 1.761(7) Å in carbon-, oxygen-, and sulfur-bridged triphenylamine.<sup>25</sup> Notably, the arrangement of OQAO and SQAO are coparallel, which is caused by C–H...O interactions (2.513 Å for OQAO, 2.682 Å for SQAO) within the horizontal direction. However, DQAO exhibits the antiparallel packing type, where the C–H...O interactions of vertical direction

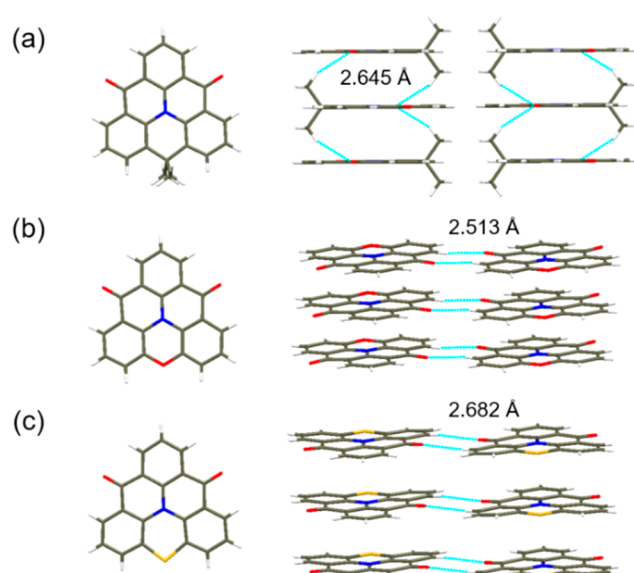


**Figure 2.** Single-crystal structure and packing mode of (a) DQAO, (b) OQAO, and (c) SQAO.

(2.645 Å) between dimethyl and carbonyl group forces the adjacent molecules to rotate 108° versus each other to maintain the  $\pi$ ... $\pi$  interactions.<sup>26</sup>

The photophysical spectroscopic properties of QAO, DQAO, OQAO, and SQAO were measured in dilute toluene solution as illustrated in Figure 3 and Table 1. All emitters

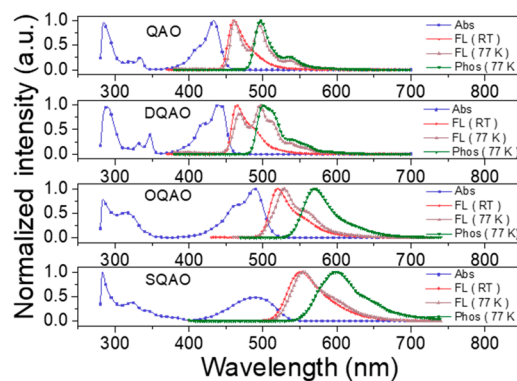


**Figure 3.** UV/vis absorption, fluorescence (298 K), fluorescence (77 K), and phosphorescence (77 K) spectra of QAO, DQAO, OQAO, and SQAO in toluene.

**Table 1.** Photophysical Properties of QAO, DQAO, OQAO, and SQAO

	$\lambda_{\text{abs}}^a$ (nm)	$\lambda_{\text{em}}^a$ (nm)	fwhm <sup>a</sup> (nm)	Stokes shift <sup>b</sup> (cm <sup>-1</sup> )	$S_1^c$ (eV)	$T_1^c$ (eV)	$\Delta E_{\text{ST}}^c$ (eV)
QAO	433	460	33	1356	2.69	2.49	0.20
DQAO	440	465	33	1222	2.66	2.47	0.19
OQAO	489	520	36	1293	2.34	2.18	0.16
SQAO	489	552	54	2334	2.23	2.07	0.16

<sup>a</sup>In toluene (10<sup>-5</sup> M) solution at room temperature. <sup>b</sup>Determined from the  $\lambda$  of UV absorption and fluorescence spectra measured in toluene solution at room temperature. <sup>c</sup>Determined from the  $\lambda$  of fluorescence and phosphorescence spectra measured in toluene solution at 77 K, respectively.

show two major absorption bands, the high energy one below 375 nm can be originated from the  $\pi-\pi^*$  and  $n-\pi^*$  transitions of the conjugated skeleton, and the longer wavelength absorption bands could be assignable to the HOMO–LUMO transitions. The photoluminescence (PL) and the absorption spectrum of the three QAO variants follow the mirror image rule, and their Stokes shifts are small (ca. 1222–2334  $\text{cm}^{-1}$ ) as expected, embodying a singlet emission event and the rigidity enforced by the fully structural constraint, preventing nonradiative channeling of excitation energy. It is noteworthy that three emitters exhibit narrow emissions at 465, 520, and 552 nm, with the fwhm as small as 0.17–0.22 eV (corresponding to 33–54 nm). From the maximum and the onset of each low-temperature spectrum (Figure 3), the  $\Delta E_{\text{ST}}$  of three emitters were calculated to be 0.19, 0.16, and 0.16 eV, respectively. To further explore the transition characteristics of the excited state, we measured the UV–vis absorption and PL spectra of four compounds in different solvents at room temperature (Figures S29 and S30). With the environmental polarity increased from nonpolar hexane to the highest polar acetone, the absorption profiles of QAO, DQAO, and OQAO change a little, while the PL spectra are more sensitive to different solvents.<sup>27</sup> SQAO displays the most significant solvatochromic effect of its fluorescent emission, and the obvious bathochromic shifts was observed from green (509 nm) in *n*-hexane to orange (601 nm) in DMF, agreeing well with its smallest HOMO/LUMO overlap integral in the calculation (Table S7) and reflecting SQAO's stronger ICT process than that of DQAO and OQAO.<sup>28</sup>

Figure S31 shows the PL spectra of three emitters in neat films (Table S9). The maximum emission peaks of DQAO, OQAO, and SQAO were observed at 482, 546, and 604 nm, accompanying a significant bathochromic shift and fwhms broadening (versus their emission bands in toluene solution). Figure S32 shows how for the doped films of 8 wt % DQAO in 1,3-bis(9*H*-carbazol-9-yl)benzene (*m*CP), 5 wt % OQAO in 4,4'-bis(9*H*-carbazol-9-yl)biphenyl (CBP), and 1 wt % SQAO in 9-(3-(9*H*-carbazol-9-yl)phenyl)-9*H*-carbazole-3-carbonitrile (*m*CPCN). This concentration was chosen to avoid aggregation of three emitters, and the absolute PLQY of the doped films was measured to be 59.3% for DQAO, 90.2% for OQAO, and 65.4% for SQAO, respectively. As shown in Figure S33, three emitters show microsecond-scale delayed component with a lifetime of 110.58  $\mu\text{s}$  for DQAO, 204.65  $\mu\text{s}$  for OQAO, and 78.38  $\mu\text{s}$  for SQAO, demonstrating their apparent TADF characteristics.

Benefiting from the rigid conformation, as shown in Figure S34 and Table S9, DQAO, OQAO, and SQAO exhibited good thermal stability with a high decomposition temperature ( $T_d$ , corresponding to 5% weight loss) of 316, 353, and 368 °C. The electrochemical behaviors were investigated by cyclic voltammetry (CV) in dichloromethane solution coated on a platinum electrode (Figure S35). Upon introduction of different electron-donating groups, the significantly distinct oxidation potentials are observed ( $E_{\text{ox}, 1/2} = 1.76$  for DQAO, 1.50 for OQAO, and 1.31 V for SQAO), and the  $E_{\text{HOMO}}$  values are calculated to be  $-5.96$ ,  $-5.70$ , and  $-5.51$  eV for DQAO, OQAO, and SQAO, respectively. Similarly, originating from the analogous half-wave reduction potentials ( $E_{\text{red}, 1/2}$ ), the  $E_{\text{LUMO}}$  values are calculated to be  $-2.90$ / $-2.93$ / $-2.95$  eV for DQAO, OQAO, and SQAO, respectively.

We performed the DFT and TD-DFT calculations at the B3LYP/6-31G(d) level to better understand the geometrical

differences and photophysical properties of the three compounds. As shown in Figure 4 and Table S7, the

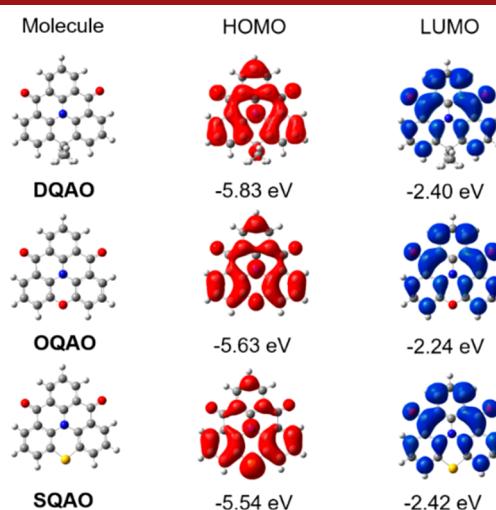
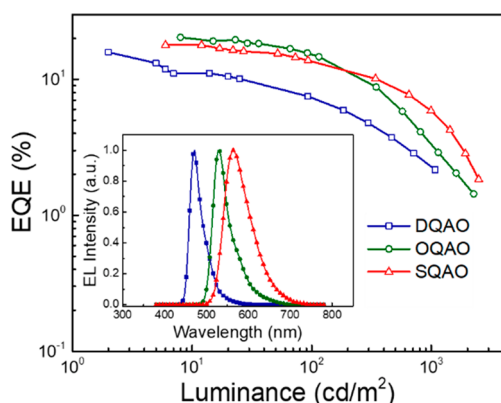


Figure 4. Density functional theory (DFT) simulations of DQAO, OQAO, and SQAO.

HOMO electron clouds of DQAO are mainly concentrated on the third bridging atoms, nitrogen atom, and its *ortho*- and *para*-carbons relative to it, whereas the LUMOs are located on the carbonyl groups and at the *meta*-carbons relative to the nitrogen atom, which revealed the short-range intramolecular charge transfer process between the nitrogen atom and carbonyl group.<sup>13,15</sup> This multiple resonance effect reduces the vibronic coupling and vibrational relaxation in the molecules, thereby achieving efficient and narrow emission.<sup>14</sup> In addition, the situation is further complicated by enhancing the electron-donating ability of the third bridging atoms, and the HOMO electron clouds has the obvious tendency of delocalization toward the third bridging position, reflecting the reinforcement of ICT character, which weakens the MR effect originated from the nitrogen atoms and carbonyl groups. For three molecules, the distributions of LUMO are similar, which agrees well with the result of electrochemical characterization.

To evaluate the function of DQAO, OQAO, and SQAO in devices, we fabricated and optimized the TADF-based OLEDs (Figure S36). The energy level alignment diagrams and current density–voltage–luminance ( $J$ – $V$ – $L$ ) of the device are displayed in Figures S37–S39. The EL spectra and EQE versus  $L$  plots of the devices are displayed in Figure 5, and the pertinent parameters are listed in Tables S10–S12. For devices with DQAO, OQAO, and SQAO, blue emission of 472 nm, green emission of 532 nm, and yellow emission of 564 nm were achieved, corresponding to Commission Internationale de l'Éclairage (CIE) coordinates of (0.12, 0.18), (0.32, 0.65), and (0.47, 0.52), respectively. Notably, the DQAO- and OQAO-based OLED exhibited the extremely narrow fwhms of 34 and 45 nm, and OLED employing DQAO only showed  $\text{EQE}_{\text{max}}$  of 15.2% and power efficiency ( $\text{PE}_{\text{max}}$ ) of 23.0  $\text{lm W}^{-1}$ . In addition, SQAO achieved an  $\text{EQE}_{\text{max}}$  of 17.8% with yellow emission, but the fwhm was much wider than DQAO and OQAO, which may due to the large radius of the sulfur atom making the molecular structure flabby. Ultimately, the device employing OQAO exhibited maximum current efficiency ( $\text{CE}_{\text{max}}$ ),  $\text{PE}_{\text{max}}$  and  $\text{EQE}_{\text{max}}$  of 26.2  $\text{cd A}^{-1}$ , 31.6  $\text{lm W}^{-1}$ ,



**Figure 5.** OLED data for DQAO, OQAO, and SQAO (electroluminescent spectra and EQE versus luminance).

and 20.3%, better than that of the device employing DQAO and SQAO because of its higher PLQY (90.2%).

In summary, we introduced three bridged-triphenylamine derivatives DQAO, OQAO, and SQAO with TADF nature, and their electronic and photophysical properties can be adjusted by tuning the substituent at the bridging positions. Encouragingly, the OLED employing DQAO, OQAO, and SQAO emitters exhibited high EQE<sub>max</sub> of 15.2%, 20.3%, and 17.8%, respectively. In particular, the fwhm of DQAO (34 nm) and OQAO (45 nm) are narrow in OLEDs, indicating its potential in commercial display. Moreover, by varying the electron-donating ability of the substituent, the emission wavelength can be facily tuned from blue (472 nm) to green (532 nm) then to the yellow area (564 nm).

## ■ ASSOCIATED CONTENT

### SI Supporting Information

The Supporting Information is available free of charge at <https://pubs.acs.org/doi/10.1021/acs.orglett.0c04159>.

Experimental details, thermal properties, electrochemical properties, UV–vis spectra, DFT calculation, single crystal, device structure, NMR spectra, and reference (PDF)

## Accession Codes

CCDC 2026180, 2026182, and 2026947 contain the supplementary crystallographic data for this paper. These data can be obtained free of charge via [www.ccdc.cam.ac.uk/data\\_request/cif](http://www.ccdc.cam.ac.uk/data_request/cif), or by emailing [data\\_request@ccdc.cam.ac.uk](mailto:data_request@ccdc.cam.ac.uk), or by contacting The Cambridge Crystallographic Data Centre, 12 Union Road, Cambridge CB2 1EZ, UK; fax: +44 1223 336033.

## ■ AUTHOR INFORMATION

### Corresponding Authors

**Zuo-Quan Jiang** – Institute of Functional Nano & Soft Materials (FUNSOM), Jiangsu Key Laboratory for Carbon-Based Functional Materials & Devices, Joint International Research Laboratory of Carbon-Based Functional Materials and Devices, Soochow University, Suzhou 215123, Jiangsu, P.R. China; [orcid.org/0000-0003-4447-2408](https://orcid.org/0000-0003-4447-2408); Email: [zqjiang@suda.edu.cn](mailto:zqjiang@suda.edu.cn)

**Liang-Sheng Liao** – Institute of Functional Nano & Soft Materials (FUNSOM), Jiangsu Key Laboratory for Carbon-Based Functional Materials & Devices, Joint International

Research Laboratory of Carbon-Based Functional Materials and Devices, Soochow University, Suzhou 215123, Jiangsu, P.R. China; [orcid.org/0000-0002-2352-9666](https://orcid.org/0000-0002-2352-9666); Email: [lsiao@suda.edu.cn](mailto:lsiao@suda.edu.cn)

## Authors

**Sheng-Nan Zou** – Institute of Functional Nano & Soft Materials (FUNSOM), Jiangsu Key Laboratory for Carbon-Based Functional Materials & Devices, Joint International Research Laboratory of Carbon-Based Functional Materials and Devices, Soochow University, Suzhou 215123, Jiangsu, P.R. China

**Chen-Chen Peng** – Institute of Functional Nano & Soft Materials (FUNSOM), Jiangsu Key Laboratory for Carbon-Based Functional Materials & Devices, Joint International Research Laboratory of Carbon-Based Functional Materials and Devices, Soochow University, Suzhou 215123, Jiangsu, P.R. China

**Sheng-Yi Yang** – Institute of Functional Nano & Soft Materials (FUNSOM), Jiangsu Key Laboratory for Carbon-Based Functional Materials & Devices, Joint International Research Laboratory of Carbon-Based Functional Materials and Devices, Soochow University, Suzhou 215123, Jiangsu, P.R. China

**Yang-Kun Qu** – Institute of Functional Nano & Soft Materials (FUNSOM), Jiangsu Key Laboratory for Carbon-Based Functional Materials & Devices, Joint International Research Laboratory of Carbon-Based Functional Materials and Devices, Soochow University, Suzhou 215123, Jiangsu, P.R. China; [orcid.org/0000-0003-0241-308X](https://orcid.org/0000-0003-0241-308X)

**You-Jun Yu** – Institute of Functional Nano & Soft Materials (FUNSOM), Jiangsu Key Laboratory for Carbon-Based Functional Materials & Devices, Joint International Research Laboratory of Carbon-Based Functional Materials and Devices, Soochow University, Suzhou 215123, Jiangsu, P.R. China

**Xing Chen** – Institute of Functional Nano & Soft Materials (FUNSOM), Jiangsu Key Laboratory for Carbon-Based Functional Materials & Devices, Joint International Research Laboratory of Carbon-Based Functional Materials and Devices, Soochow University, Suzhou 215123, Jiangsu, P.R. China

Complete contact information is available at: <https://pubs.acs.org/doi/10.1021/acs.orglett.0c04159>

## Author Contributions

<sup>‡</sup>S.-N.Z. and C.-C.P. contributed equally.

## Notes

The authors declare no competing financial interest.

## ■ ACKNOWLEDGMENTS

We acknowledge financial support from the National Natural Science Foundation of China (Nos. 61961160731, 51773141, and 51873139) and the Natural Science Foundation of Jiangsu Province of China (BK20181442). This project is also funded by Collaborative Innovation Center of Suzhou Nano Science & Technology, the Priority Academic Program Development of Jiangsu Higher Education Institutions (PAPD), the 111 Project of The State Administration of Foreign Experts Affairs of China.

## ■ REFERENCES

- (1) Hirai, M.; Tanaka, N.; Sakai, M.; Yamaguchi, S. Structurally Constrained Boron-, Nitrogen-, Silicon-, and Phosphorus-Centered Polycyclic  $\pi$ -Conjugated Systems. *Chem. Rev.* **2019**, *119*, 8291–8331.
- (2) Wakamiya, A.; Nishimura, H.; Fukushima, T.; Suzuki, F.; Saeki, A.; Seki, S.; Osaka, I.; Sasamori, T.; Murata, M.; Murata, Y.; Kaji, H. On-Top  $\pi$ -Stacking of Quasiplanar Molecules in Hole-Transporting Materials: Inducing Anisotropic Carrier Mobility in Amorphous Films. *Angew. Chem., Int. Ed.* **2014**, *53*, 5800–5804.
- (3) Nishimura, H.; Ishida, N.; Shimazaki, A.; Wakamiya, A.; Saeki, A.; Scott, L. T.; Murata, Y. Hole-Transporting Materials with a Two-Dimensionally Expanded  $\pi$ -System around an Azulene Core for Efficient Perovskite Solar Cells. *J. Am. Chem. Soc.* **2015**, *137*, 15656–15659.
- (4) Choi, H.; Park, S.; Paek, S.; Ekanayake, P.; Nazeeruddin, M. K.; Ko, J. Efficient star-shaped hole transporting materials with diphenylethynyl side arms for an efficient perovskite solar cell. *J. Mater. Chem. A* **2014**, *2*, 19136–19140.
- (5) Nishimura, H.; Tanaka, K.; Morisaki, Y.; Chujo, Y.; Wakamiya, A.; Murata, Y. Oxygen-Bridged Diphenyl-naphthylamine as a Scaffold for Full-Color Circularly Polarized Luminescent Materials. *J. Org. Chem.* **2017**, *82*, 5242–5249.
- (6) Nishimura, H.; Fukushima, T.; Wakamiya, A.; Murata, Y.; Kaji, H. The Influence of Quasiplanar Structures of Partially Oxygen-Bridged Triphenylamine Dimers on the Properties of Their Bulk Films. *Bull. Chem. Soc. Jpn.* **2016**, *89*, 726–732.
- (7) Jiang, Z.; Ye, T.; Yang, C.; Yang, D.; Zhu, M.; Zhong, C.; Qin, J.; Ma, D. Star-Shaped Oligotriarylamines with Planarized Triphenylamine Core: Solution-Processable, High- $T_g$  Hole-Injecting and Hole-Transporting Materials for Organic Light-Emitting Devices. *Chem. Mater.* **2011**, *23*, 771–777.
- (8) Hellwinkel, D.; Melan, M. 8.12-Dihydro-4H-benzo[1.9]-chinolinizin[3.4.5.6.7-defg]acridin-trion-(4.8.12) und 5.9-Dihydro-chino[3.2.1-de]acridin-dion-(5.9). *Chem. Ber.* **1971**, *104*, 1001–1016.
- (9) Field, J. E.; Venkataraman, D. Heterotriangulenes-Structure and Properties. *Chem. Mater.* **2002**, *14*, 962–964.
- (10) Hellwinkel, D.; Melan, M. Zur Stereochemie verbrückter Triarylamine. *Chem. Ber.* **1974**, *107*, 616–626.
- (11) Field, J. E.; Hill, T. J.; Venkataraman, D. Bridged Triarylamines: A New Class of Heterohelices. *J. Org. Chem.* **2003**, *68*, 6071–6078.
- (12) Kuratsu, M.; Kozaki, M.; Okada, K. 2,2':6',6'-Trioxy-triphenylamine: Synthesis and Properties of the Radical Cation and Neutral Species. *Angew. Chem.* **2005**, *117*, 4124–4126.
- (13) Yuan, Y.; Tang, X.; Du, X. Y.; Hu, Y.; Yu, Y. J.; Jiang, Z. Q.; Liao, L. S.; Lee, S. T. The Design of Fused Amine/Carbonyl System for Efficient Thermally Activated Delayed Fluorescence: Novel Multiple Resonance Core and Electron Acceptor. *Adv. Opt. Mater.* **2019**, *7*, 1801536.
- (14) Kondo, Y.; Yoshiura, K.; Kitera, S.; Nishi, H.; Oda, S.; Gotoh, H.; Sasada, Y.; Yanai, M.; Hatakeyama, T. Narrowband deep-blue organic light-emitting diode featuring an organoboron-based emitter. *Nat. Photonics* **2019**, *13*, 678–682.
- (15) Hatakeyama, T.; Shiren, K.; Nakajima, K.; Nomura, S.; Nakatsuka, S.; Kinoshita, K.; Ni, J.; Ono, Y.; Ikuta, T. Ultrapure Blue Thermally Activated Delayed Fluorescence Molecules: Efficient HOMO–LUMO Separation by the Multiple Resonance Effect. *Adv. Mater.* **2016**, *28*, 2777–2781.
- (16) Oda, S.; Kawakami, B.; Kawasumi, R.; Okita, R.; Hatakeyama, T. Multiple Resonance Effect-Induced Sky-Blue Thermally Activated Delayed Fluorescence with a Narrow Emission Band. *Org. Lett.* **2019**, *21*, 9311–9314.
- (17) Madayanad Suresh, S.; Hall, D.; Beljonne, D.; Olivier, Y.; Zysman-Colman, E. Multiresonant Thermally Activated Delayed Fluorescence Emitters Based on Heteroatom-Doped Nanographenes: Recent Advances and Prospects for Organic Light-Emitting Diodes. *Adv. Funct. Mater.* **2020**, *30*, 1908677.
- (18) Sun, D.; Suresh, S. M.; Hall, D.; Zhang, M.; Si, C.; Cordes, D. B.; Slawin, A. M. Z.; Olivier, Y.; Zhang, X.; Zysman-Colman, E. The design of an extended multiple resonance TADF emitter based on a polycyclic amine/carbonyl system. *Mater. Chem. Front.* **2020**, *4*, 2018–2022.
- (19) Zhang, Y.; Zhang, D.; Wei, J.; Liu, Z.; Lu, Y.; Duan, L. Multi-Resonance Induced Thermally Activated Delayed Fluorophores for Narrowband Green OLEDs. *Angew. Chem., Int. Ed.* **2019**, *58*, 16912–16917.
- (20) Xu, Y.; Li, C.; Li, Z.; Wang, Q.; Cai, X.; Wei, J.; Wang, Y. Constructing Charge-Transfer Excited States Based on Frontier Molecular Orbital Engineering: Narrowband Green Electroluminescence with High Color Purity and Efficiency. *Angew. Chem., Int. Ed.* **2020**, *59*, 17442–17446.
- (21) Zhang, Y.; Zhang, D.; Wei, J.; Hong, X.; Lu, Y.; Hu, D.; Li, G.; Liu, Z.; Chen, Y.; Duan, L. Achieving Pure Green Electroluminescence with CIE<sub>y</sub> of 0.69 and EQE of 28.2% from an Aza-Fused Multi-Resonance Emitter. *Angew. Chem., Int. Ed.* **2020**, *59*, 17499–17503.
- (22) Yang, M.; Park, I.; Yasuda, T. Full-Color, Narrowband, and High-Efficiency Electroluminescence from Boron and Carbazole Embedded Polycyclic Heteroaromatics. *J. Am. Chem. Soc.* **2020**, *142*, 19468–19472.
- (23) Stoyanovich, F. M.; Marakatkina, M. A. The Di-metalation of 9-Phenylcarbazole. *Izv. Akad. Nauk SSSR Ser. Khim.* **1978**, *150*, 1729–1733.
- (24) Hall, D.; Suresh, S. M.; dos Santos, P. L.; Duda, E.; Bagnich, S.; Pershin, A.; Rajamalli, P.; Cordes, D. B.; Slawin, A. M. Z.; Beljonne, D.; Köhler, A.; Samuel, I. D. W.; Olivier, Y.; Zysman-Colman, E. Improving Processability and Efficiency of Resonant TADF Emitters: A Design Strategy. *Adv. Opt. Mater.* **2020**, *8*, 1901627.
- (25) Nakatsuka, S.; Gotoh, H.; Kinoshita, K.; Yasuda, N.; Hatakeyama, T. Divergent Synthesis of Heteroatom-Centered 4,8,12-Triazatriangulenes. *Angew. Chem., Int. Ed.* **2017**, *56*, 5087–5090.
- (26) Hamzehpoor, E.; Perepichka, D. F. Crystal Engineering of Room Temperature Phosphorescence in Organic Solids. *Angew. Chem., Int. Ed.* **2020**, *59*, 9977–9981.
- (27) Li, X.; Shi, Y. Z.; Wang, K.; Zhang, M.; Zheng, C. J.; Sun, D. M.; Dai, G. L.; Fan, X. C.; Wang, D. Q.; Liu, W.; Li, Y. Q.; Yu, J.; Ou, X. M.; Adachi, C.; Zhang, X. H. Thermally Activated Delayed Fluorescence Carbonyl Derivatives for Organic Light-Emitting Diodes with Extremely Narrow Full Width at Half-Maximum. *ACS Appl. Mater. Interfaces* **2019**, *11*, 13472–13480.
- (28) Matsui, K.; Oda, S.; Yoshiura, K.; Nakajima, K.; Yasuda, N.; Hatakeyama, T. One-Shot Multiple Borylation toward BN-Doped Nanographenes. *J. Am. Chem. Soc.* **2018**, *140*, 1195–1198.